

AUG 64

## PHOTOMETRY OF THE EARTH FROM MARINER II \*T

Robert L. Wildey

Division of Geological Sciences and  
Mount Wilson and Palomar Observatories,  
California Institute of Technology and  
Carnegie Institution of Washington

FACILITY FORM 602	N65-24729	(THRU)
	22	31
	CR-63097	30
	(ACCESSION NUMBER)	(CODE)
	(PAGES)	(CATEGORY)
	(NASA CR OR TMX OR AD NUMBER)	

GPO PRICE \$ \_\_\_\_\_

OTS PRICE(S) \$ \_\_\_\_\_

Hard copy (HC) 1.00Microfiche (MF) .50

\* The access to the telemetry record which provides the data for this study is by courtesy of the Jet Propulsion Laboratory, California Institute of Technology, Pasadena, California.

T Contribution No. 1264 of the Division of Geological Sciences, California Institute of Technology, Pasadena, California.

# ABSTRACT

24729  
The Earth tracking system aboard the Mariner II spacecraft has collected photometric observations of the Earth as a by-product of its navigational duties on the flight to Venus. The observations show good agreement with the phase curve for the Earth that was previously found by observing the earth-lit moon. Diurnal variations in brightness are correlated with the fraction of the Earth's disk covered by land.

*Author*

Introduction. All previous photometric studies of the total visual flux (i.e. integrated over the apparent disk) of the earth have been made by measuring the brightness of that portion of the moon which is illuminated only by sunlight that has been reflected from the earth. The classical work in this field has been that of Danjon (1954), using the "cat-eye" photometer, and is the source of the presently accepted value of the albedo of the earth. Such measurements are based on a visual nulling of the brightness-suppressed sunlit portion of the moon against the unsuppressed earthlit portion. The amount of suppression, accurately known, constitutes the fundamental datum. It is then necessary to make a completely independent set of comparisons of the sunlit moon with a constant source, usually the sun, before an absolute visual flux for the earth can be obtained. Danjon's method solves quite well the problem of atmospheric extinction.

There are three principal difficulties to be encountered with the use of the moon as an intermediary in doing photometry of the earth. (1) The sunlit portion is the source of considerable scattered light in the earthlit image which may make measurements systematically too high, and as one approaches full moon the amount of scattered light increases while the amount of earth-shine decreases. (2) To within rather narrow limits, the fixed location of an observatory imposes an unwanted correlation between the earth's phase angle, as seen from the moon, and the geographic longitude and latitude of the sublunar point. The latitude bias thus introduced in the earth's phase curve can be investigated by examining<sup>n</sup> the observations for seasonal variations. Although the longitude effects can be investigated by making measurements from observatories well distributed over the earth's surface, such observations have been previously collected only in France. A restrictive corollary of this effect is that the earth's phase angle cannot be held constant while the geography presented upon its disk is varied and any implied brightness changes are measured. (3) The lunar neighborhoods on opposite sides of the terminator that are intercompared may possess intrinsic sources of

brightness difference which would be present even under illumination by the same flux. They may differ slightly in normal albedo, and must also possess differences, of varying magnitude, due to the non-degeneracy of the moon's photometric function in any of its three degrees of freedom.

Such difficulties are alleviated when one does photometry of the earth from space. Such observations are the useful by-product of the Mariner - II spacecraft's guidance instrumentation.

Observations. The reduceable data were collected during the 52 day period from September 29 to November 22, 1962. Prior to the earlier date the telemetry indicated an abnormally low signal by nearly a factor of 100, the explanation for which remains elusive. Recovery was sudden and was followed by indications of normal operation. Later than November 22, the temperature, which had been rising rapidly, was too high to be corrected for in the data reduction. It will be seen that the method of correction for the temperature dependence of responsivity begins to fail toward the latter part of the 52 day period.

The photometer used to collect these observations constitutes one aspect of the the Long Range Earth Sensor (LRES). This device has been described in detail by G. W. Meisenholder in the internal publications of the Jet Propulsion Laboratory (SPS 37-6, -9, -14, and -16, Vol. II) and by McLauchlan (1964). Inasmuch as these reports are of limited edition, a short redescription will be given.

The LRES uses a single, end-on, 3/4 -in. diameter, S - II photocathode Dumont photomultiplier tube whose field is limited by a fine aperture stop. Both stop and detector are behind the focal plane. Coincident at all times with the focal plane is a modulating mask attached to a 22 cps vibrating read. Ahead of the modulating mask is a fixed aperture, preceded in the optical train by the objective, which is a 7 - element f1.2 lens of 2 inch focal length. The purpose of the LRES is to provide information regarding orientation in space for the purpose of performing navigational and orientational

maneuvers. In this function the photomultiplier tube serves only as a light detector and has no position discrimination by itself.

The vibrating reed moves through a sufficient arc so that the modulating mask completely uncovers the fixed aperture at the extremes of motion. The photoelectric output, therefore, is a series of pulses. The shapes of the knife edges of the modulating mask are such that a shift of the position of the Earth image in hinge causes a variation in the output pulse width, while a shift in roll causes a variation in phase (or time) of the photoelectric output relative to the reed motion. These properties of the output waveform are detected and provide dc error signals for attitude correction. Also present in the output are signals which indicate that an object is being tracked by the sensor and the amount of light being sensed.

The threshold of the unit is approximately  $5 \times 10^{-11} \text{ W/CM}^2$  (blackbody bolometric at  $6000^\circ\text{K}$ ) and the maximum permissible sustained signal is  $5 \times 10^{-7} \text{ W/CM}^2$ .

The photometer signal was calibrated, relatively, over the entire dynamic range to be encountered on the mission, by use of an earth simulator. Absolute calibration was obtained with the aid of a National Bureau of Standards lamp. No in-flight calibration existed. The foot-candle (ft-cd) has been chosen as the unit in which to express the results of the photometry. It is a standard unit and is based on a radiation bandpass that does not differ from the photometer bandpass by as much as any other logical choice except, of course, a mean monochromatic flux corresponding to the effective wavelength of the photometer. It can be readily shown that the reduction equation is exactly given by:

$$S_{\bullet} = \frac{\langle f_{\bullet}(\lambda) \rangle_V \langle f_o(\lambda) \rangle_{SII}}{\langle f_{\bullet}(\lambda) \rangle_{SII} \langle f_o(\lambda) \rangle_V} \cdot S_o \cdot R(T, 70^\circ) \cdot \frac{I_{\bullet}}{I_o} \quad (1)$$

where the subscript V following the expectation-value brackets denotes that the quantity within the brackets has been weighted over wavelength according to the response function of the eye (Walsh, 1953). A subscript SII implies that the weighting function has been

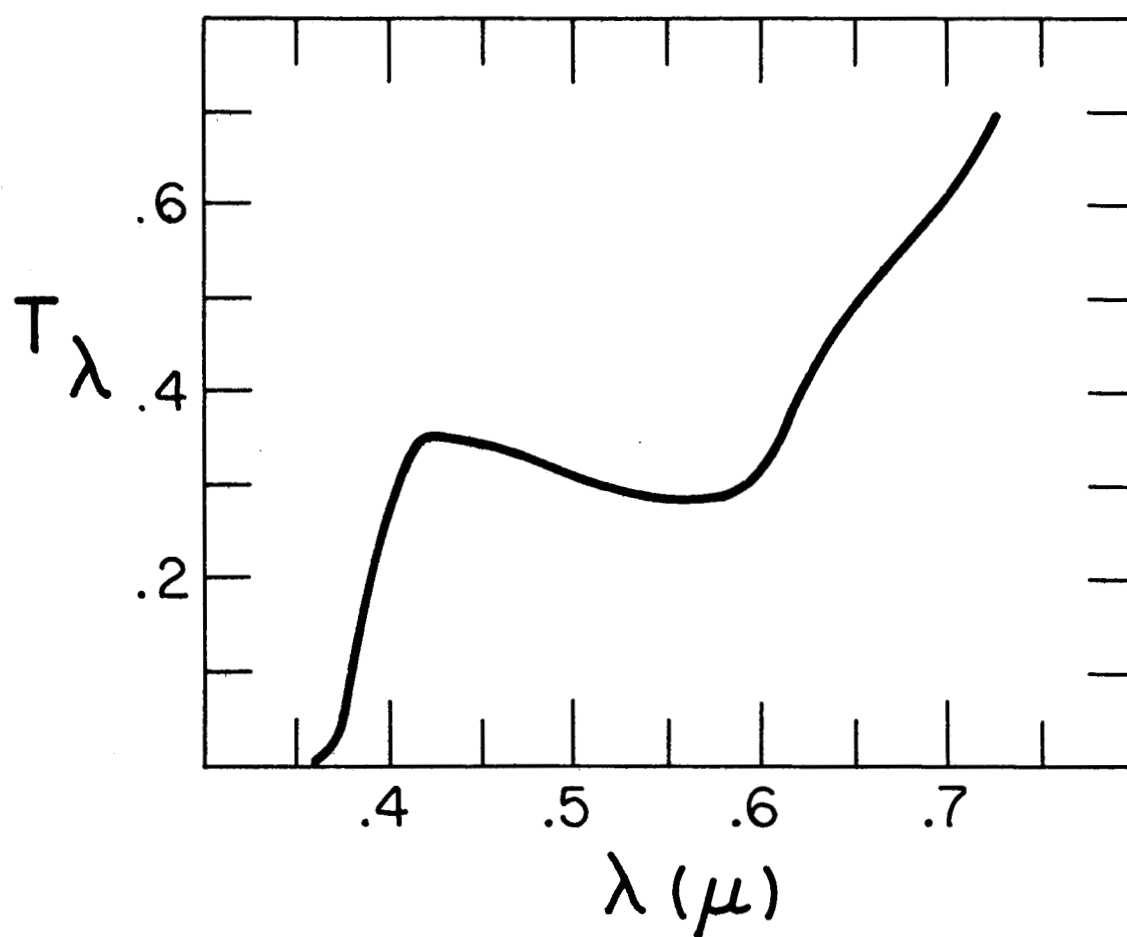


Fig. 1. Spectral transmission curve for the objective lens of the type used in Mariner II's Long Range Earth Sensor.

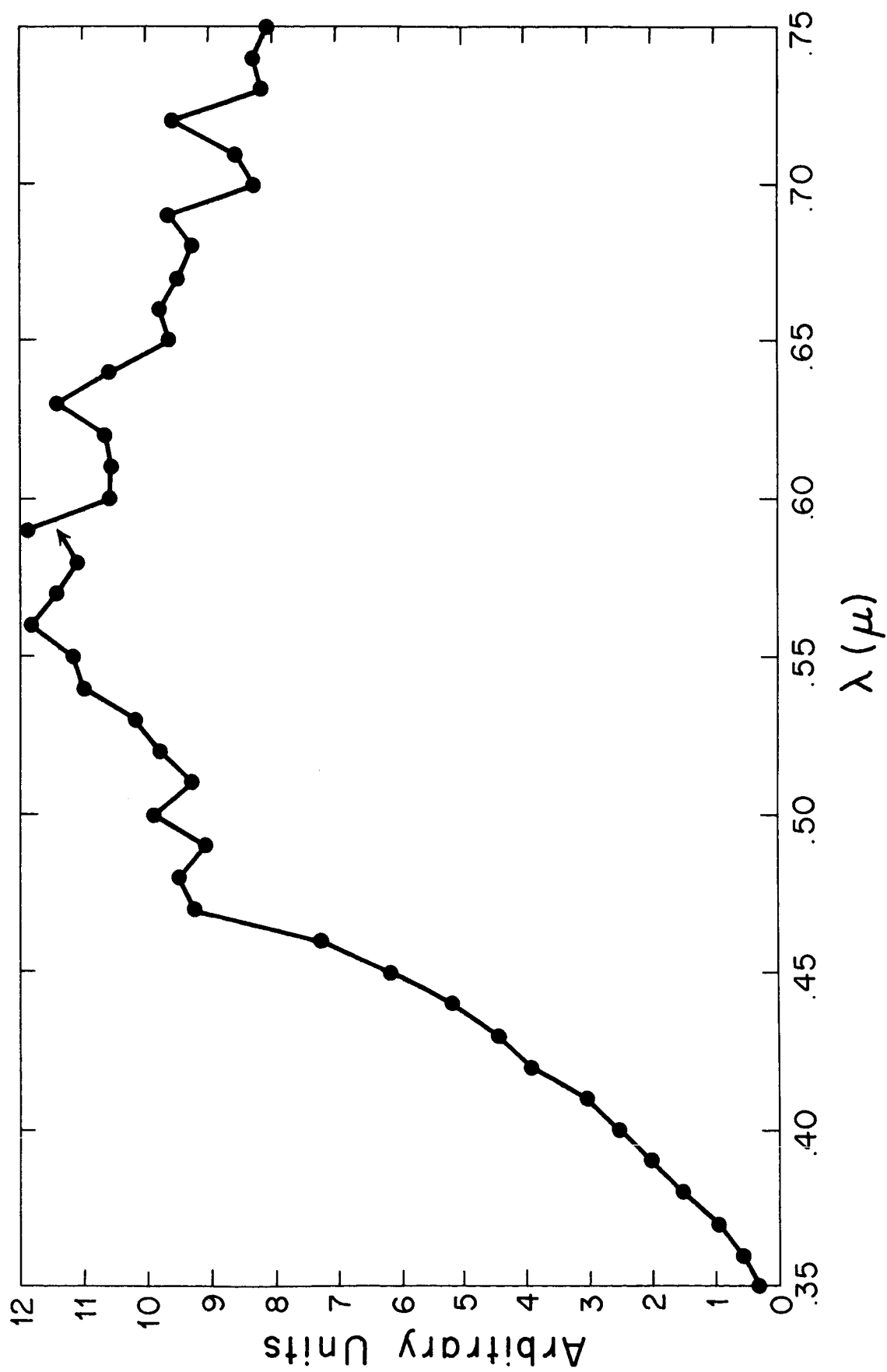


Fig. 2. Spectral energy distribution of calibration source.

multiplied by the transmission of the objective lens (Figure 1) the response of an SII photoemissive surface (Radio Corporation of America, 1958).

The quantities  $f_o(\lambda)$  and  $f_e(\lambda)$  are the spectral energy distributions, in arbitrary units, of the standard source and the earth flux, respectively.  $S_o$  is the foot-candle output of the standard source.  $R(T, 70^\circ)$  is the ratio of the response at  $70^\circ\text{F}$ , at which temperature the laboratory measurements were made, to the response at  $T$ , the temperature of the photometer at a given measuring time, which is also in the telemetry record.

$I_e$  is the photoelectric current produced by the earth flux and  $I_o$  is the photo-current produced by the standard source.

Measurements of  $f_o(\lambda)$  were undertaken in the laboratory and are shown in Figure 2.  $f_e(\lambda)$  was taken as the product of three factors. The first is the empirical solar continuum published by Minnaert (1953). The second is one minus the Fraunhofer line blanketing coefficient published by Michard (1950). The third term must allow for the wavelength dependence of the overall reflectivity of the earth. The only information bearing upon this are Danjon's 3 color observations. Danjon gives a color index (C.I.) for earthshine transformed to the magnitude-color system of Rougier (1937). He finds a seasonal variation. The median color has been adopted, which should be an optimum procedure since the sub-Mariner point was always close to the equator. A heuristic procedure was adopted to make use of this C.I. of 0.68. Rougier's C.I. of the moon shining by direct sunlight is 1.10. Thus the earth's reflectivity at the blue effective wavelength is -0.42 magnitudes, or 47.3 percent, higher than it is at the visual effective wavelength. It remains to specify the effective wavelengths. For this purpose an ordinary color equation was assumed connecting C.I. to the Johnson (1955) BV system.

$$B - V = A (C.I.) + C \quad (2)$$

Using Rougier's values of C.I. for the sun (0.79) and the moon, and values of  $B - V$  for the sun of 0.60 (Stebbins and Kron, 1957) and for the moon of 0.85 (van den Bergh, 1962; Wildey and Pohn, 1964) equation 2 was solved for  $A$ . Interpreting  $A$  in



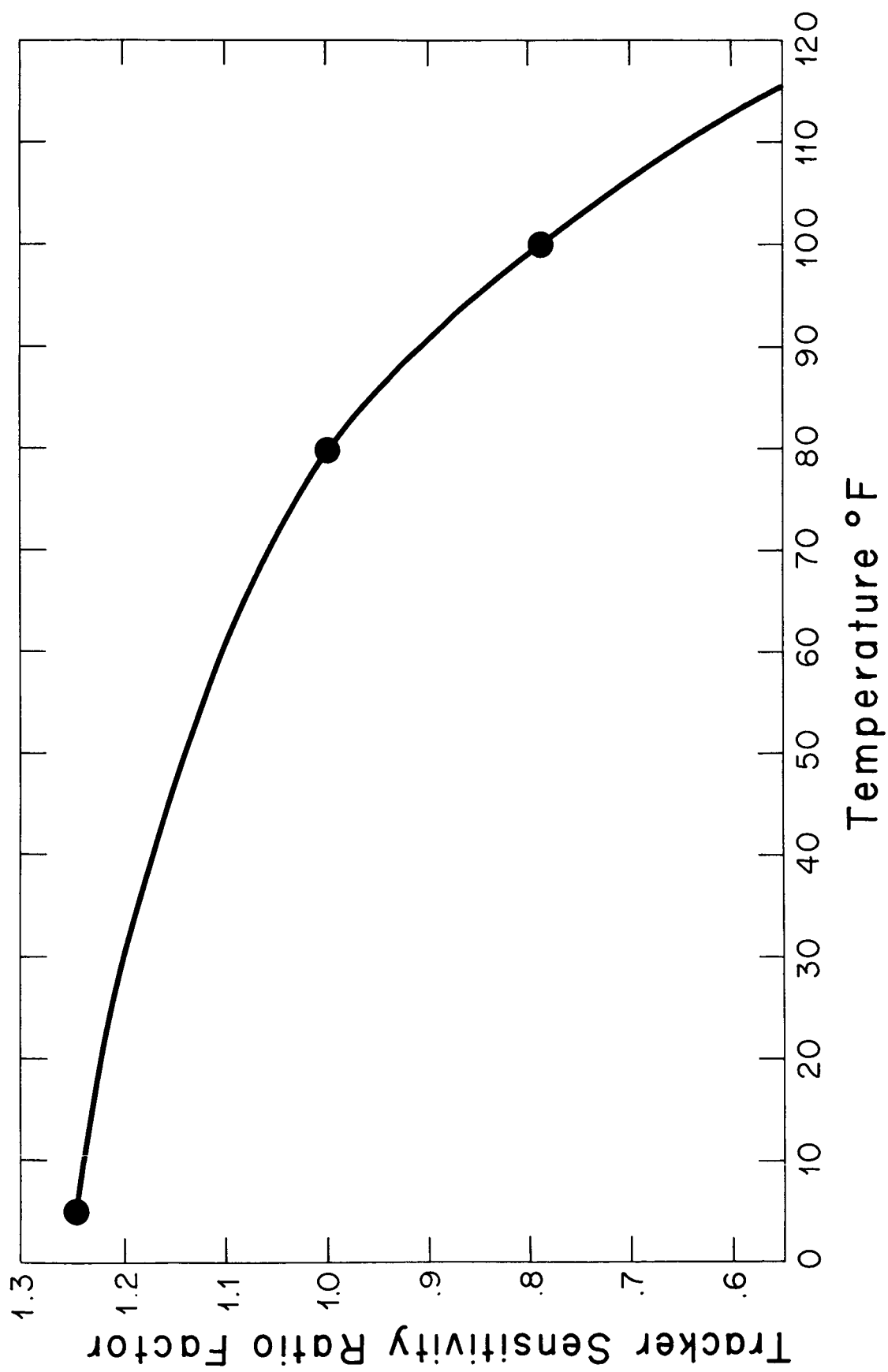


Fig . 3 . Relative response, in arbitrary units of radiative power, as a function of temperature .

terms of the wavelength baselines in the usual way (e.g. Wildey and Murray, 1964; Mathews and Sandage, 1963) and assuming the effective wavelengths of B to be  $\lambda 4430\text{\AA}$  and of both V and Rougier's yellow magnitude to be  $\lambda 5540\text{\AA}$ , the blue effective wavelength of Rougier becomes  $\lambda 4230\text{\AA}$ . The curve of the reflectivity of the earth versus wavelength was then assumed to be linear with a value of 1.47 at  $\lambda 4230\text{\AA}$  and 1.00 at  $\lambda 5540\text{\AA}$ . This source of uncertainty may imply a systematic error in the photometry of 10 or 20 percent.

Three data points were obtained in the laboratory relating photometer responsivity to temperature. They are plotted in Figure ~~X~~<sup>3</sup>. A smooth curve, whose functional form could not be specified, was fitted to these three points by eye. The accuracy of the correction provided implies it is an insignificant source of systematic error for most of the data of the present study. Barring a highly improbable interpretation of the later data, however, the temperature renders the latter part of the observations unacceptable for the study of other than diurnal brightness variations.

The possibility of the existence of other unknown sources of systematic error cannot be completely discounted in view of the unexplained behavior of the LRES signal at the beginning of the flight.

The only important source of random error is the number of significant digits carried in the telemetry and results in an uncertainty of about  $\pm 2$  percent. Extracting a tabulation of observations from the telemetry record becomes primarily a problem of identifying the recorded times when a given signal is holding fast and when the frequency of truncation between two consecutive signal numbers is equal.

The observations are tabulated in Table I. Most of the column headings are self-explanatory. Column one lists the geocentric julian day beyond 2437937. Column 7 lists the luminous flux of the earth normalized to a distance of one astronomical unit assuming an inverse square dependence. This flux has been temperature corrected.

Results. The integral brightness versus phase of the earth over the range in phase

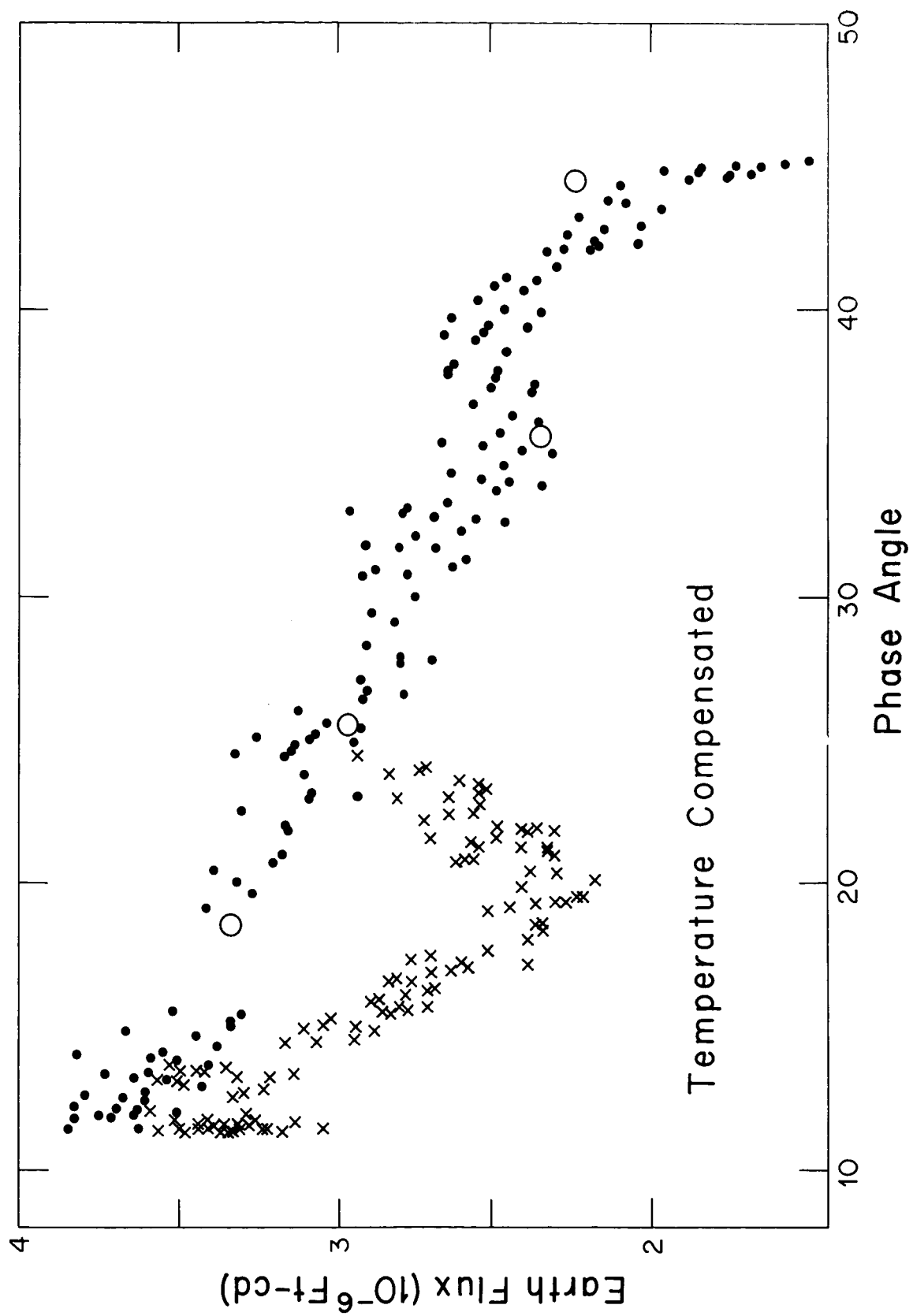


Fig . 4 . Luminous Flux of the entire visible Earth versus the angle , as seen from the Earth , between the sun and the direction of measurement . Plot has been corrected for temperature variations of the photometer .

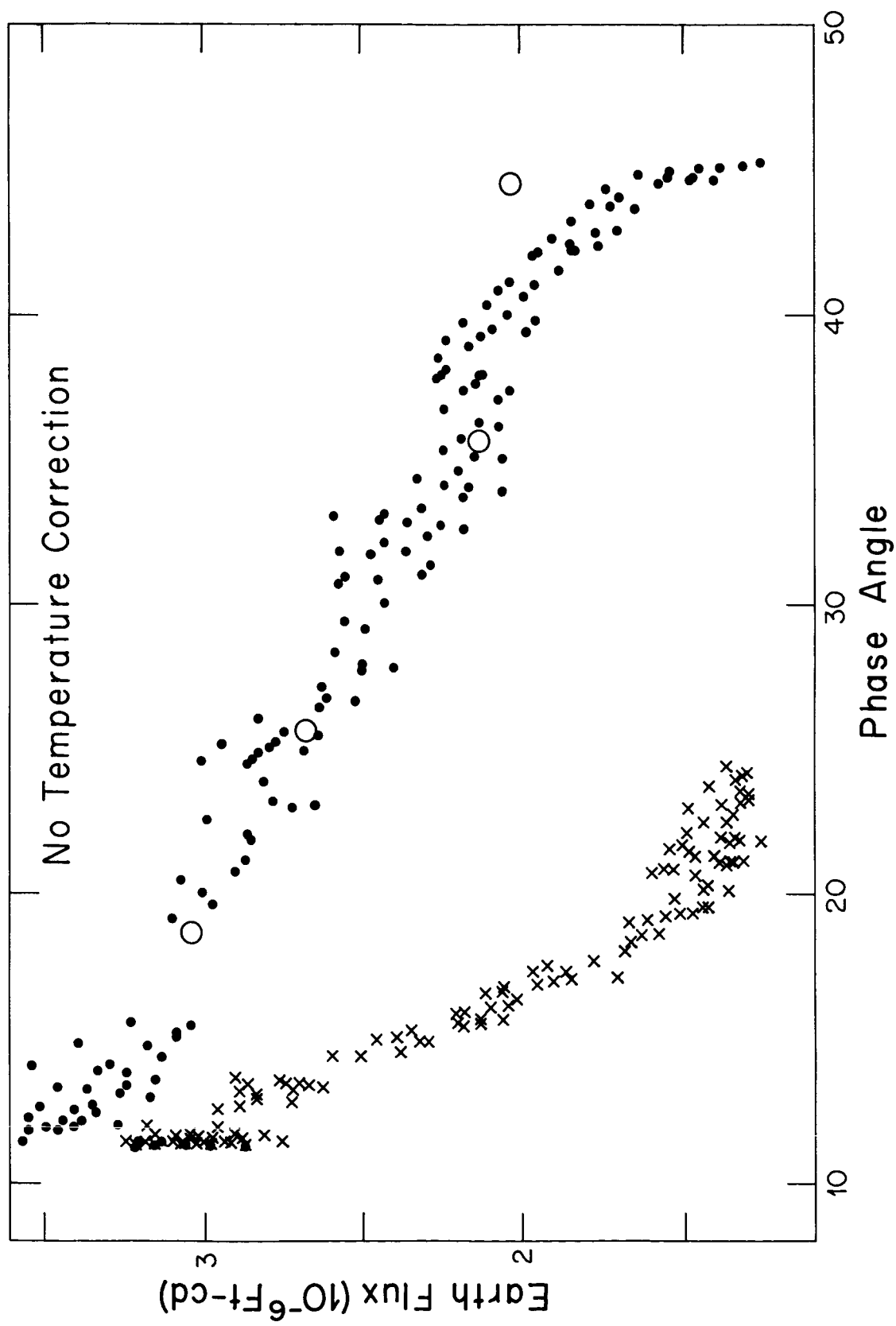


Fig. 5 . As in Figure 4 except that no correction has been made for the temperature variation between laboratory and celestial environment .

angle possible for the present study is shown in Figure ~~4~~<sup>4</sup>. Figure ~~5~~<sup>5</sup> shows, for comparison, the same plot uncorrected for temperature.

Chronologically the phase-angle decreases from the maximum  $45^\circ$  shown to the minimum indicated in the figure and then again increases. This minimum corresponds to about the time that the temperature begins to rise sharply. The failure to reproduce the phase curve recorded before minimum phase, as the Sun-Earth-Mariner angle is now increased<sup>3</sup>, is apparently a failure of Figure ~~3~~<sup>3</sup> to represent the responsivity variation at these higher temperatures.

The scatter present in the sequences of Figures ~~4~~<sup>4</sup> and ~~5~~<sup>5</sup> is merely the diurnal brightness variation whose periodicity is very short compared to the time required to produce a significant change in phase-angle.

It can be seen in Figures ~~4~~<sup>4</sup> and ~~5~~<sup>5</sup> that there is also present a semi-periodic light variation superimposed on the diurnal effect, of approximately the same or slightly larger amplitude, but with a characteristic period of about 5 to 6 days. No satisfactory explanation for this phenomenon can be offered at present.

The large open circles represent Danjon's mean curve for the Earth's integral brightness versus phase, to which has been applied a normalization scale factor to fit the present data at Danjon's minimum phase angle. Danjon's relation has the seasonal variation averaged out. It should thus correspond to the Mariner photometry which was always near zero geographic latitude, except for the longitude effect mentioned earlier. The agreement between the indirect and the direct photometry is good. Unfortunately, investigation at the larger more critical phase angles was not permitted by the trajectory. Hopefully, this important data will be provided by the LRES data collected on the Mariner B flight to Mars.

The scale factor found necessary to be applied to Danjon's data in order to produce agreement with the present measurements was  $0.482$ . In view of the size of previously investigated systematic errors and especially because the abnormal

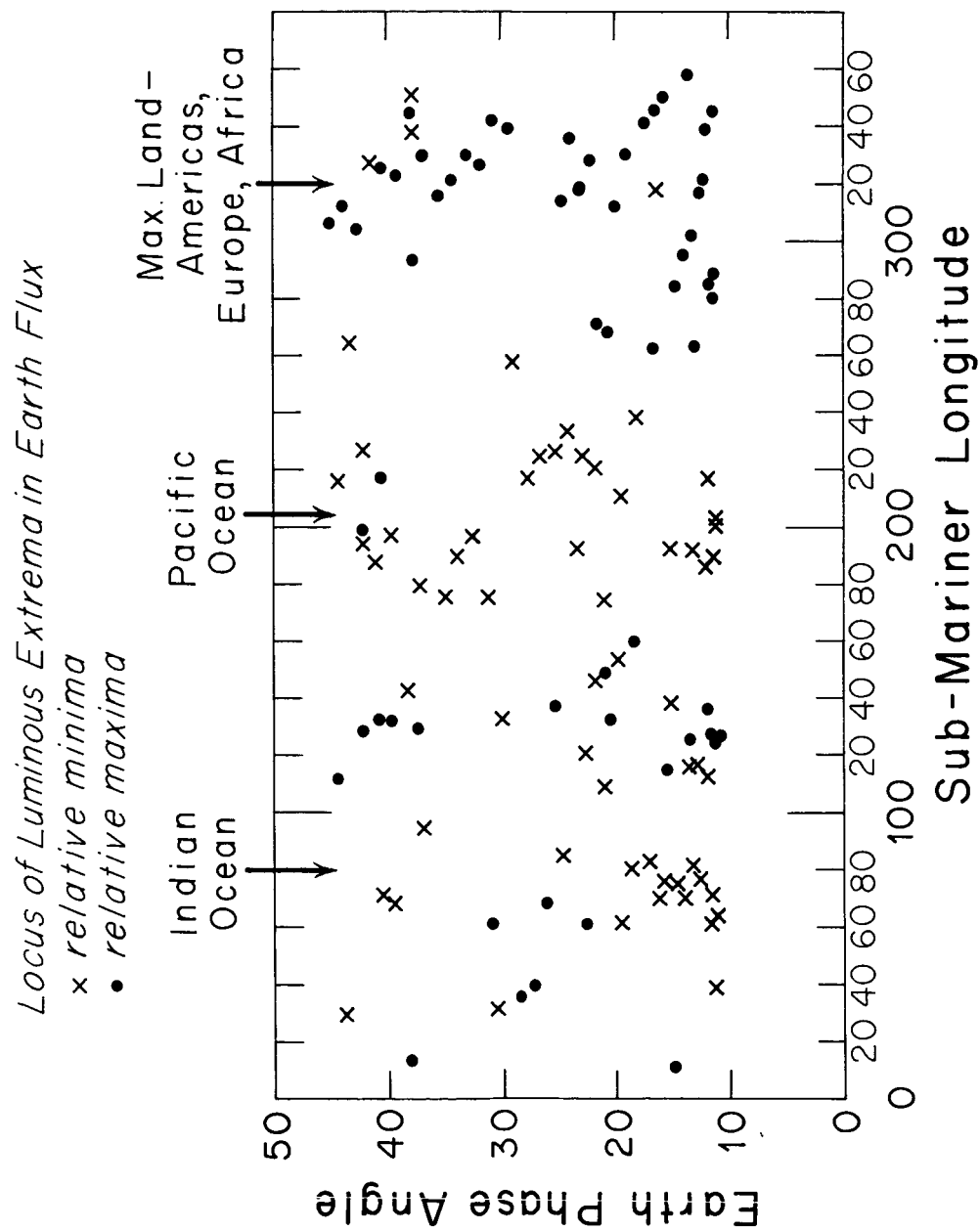


Fig. 6. Plot of the phase angle of the Earth versus the geographic longitude of the sub-Mariner point for those times when the Long Range Earth Sensor is recording a relative maximum or minimum in signal.

behavior of LRES during the early period of the flight has not been satisfactorily explained, the attachment of significance to this deviation should be viewed with caution.

Three degrees of freedom are associated with the specification of Earth's luminous flux in any kind of steady state: (1) the earth's phase angle from the direction of measurement; (2) the geographic longitude passing through that point on the Earth's surface where the direction of measurement passes through the zenith; and (3) the corresponding latitude. In the present study we may assume that the third degree of freedom has been held approximately constant. It is therefore of significance to ask what the locus of relative brightness extrema in the (Earth phase angle, sub-Mariner longitude) plane looks like. Table I has been examined for relative maxima and minima and the associated data have been plotted in Figure <sup>b</sup>~~X~~. There does not appear to be a very systematic effect associated with phase. The longitudes associated with the most pronounced maxima correspond to a point in the Atlantic Ocean above the eastern extreme of South America, and appear to correspond very nearly to a maximum in projected land-fraction. The most pronounced minima is in the center of the Pacific Ocean and represents approximately a minimum in projected land fraction.

In order to obtain an estimate of the relative reflecting power of landforms compared to ocean, the following simple analysis, which ignores any possible limb-darkening the Earth may exhibit, was undertaken. A globe of the Earth was photographed with the sub-camera point corresponding to the geographic coordinates of the sub-Mariner point for the means of each of the above two brightness extrema. The two photographs were planimetered over the entire projected disk. Thus the phase-angle was assumed zero. Table I was then examined for maximum-minimum pairs which satisfied the criteria that the maxima fall between  $280^{\circ}$  and  $360^{\circ}$  longitude and the minima fall between  $170^{\circ}$  and  $240^{\circ}$ . In addition the elements of a given pair were required to differ by less than 1.5 in phase angle. Twenty-two such pairs were found. The ratio of maximum to minimum

brightness was evaluated. This ratio appears uncorrelated with phase angle. In view of this fact and the fact that no distinct trend is exhibited against phase angle in Figure <sup>6</sup>~~X~~, the assumption of a full earth in planimetry of the photographs seems justified.

The results of the planimetry yield that the projected land fraction for the Pacific point is 0.061 while that for the Atlantic sub-Mariner point is 0.355. The mean ratio of maximum to adjacent minimum brightness is  $1.12 \pm .01$  S.D. Simple calculations then reveal that, for equal illuminated areas, average landform is  $1.41 \pm .03$  S.D. times as bright as average ocean. Water has a higher albedo than land, but is not as good a back-scatterer. Inasmuch as the range in phase angle was not too far from zero, this might be part of the explanation for these relative reflectivities. However, one would thus expect to see the ratio of maximum to minimum brightness exhibit a phase dependence, contrary to the present observations. An alternative explanation would suggest that clouds, phenomena of high albedo, tend to concentrate over land relative to water.

Two exceptional cases are noted in Figure <sup>6</sup>~~X~~ where maxima rather than minima occur over the Pacific. Meteorological reports from the vicinity at these times do not suggest exceptional cloudiness. Perhaps the ocean region from which a specular reflection of the sun is obtained was unusually becalmed. A more detailed mathematical analysis of these data entailing a running correlation with world-wide meteorological conditions and especially Tiros satellite photographs will be the subject of a later paper.

Acknowledgements. It is a pleasure to thank G. W. Meisenholder of the Jet Propulsion Laboratory for inviting the author to investigate the telemetry record. He, L. D. Runkle, M. D. Higgins, and F. G. Kurl have been of considerable assistance in obtaining the proper records. I wish to also thank J. R. Kroth for helping with the reductions. This work has been supported in part by the National Aeronautics and Space Administration under Contract NAS 7-100 and Grant NsG 56-60.

---



## REFERENCES

- Bergh, S. van den, The Color of the Moon, Astron. J., 67, 147-150, 1962.
- Danjon, A., Albedo, Color, and Polarization of the Earth, The Earth as a Planet, edited by G. P. Kuiper, University of Chicago Press, Chicago, 726-738, 1954.
- Johnson, H. L., The UBV Photometric System, Ann. d'Astrophys., 18, 292-296, 1955.
- Mathews, T. A., and A. R. Sandage, Optical Identification of 3C48, 3C196, and 3C286 with Stellar Objects, Astrophys. J., 138, 30-56, 1963.
- McLauchlin, J., Symposium on Spectroscopic Instrumentation in Extra-Terrestrial Environments, Jet Propulsion Laboratory, paper presented April 28, 1964.
- Michard, R., On the Energy Distribution in the Ultra-Violet Continuous Spectrum of the Sun, Bull. Astron. Inst. Netherlands, 11, 227-231, 1950.
- Minnaert, M., The Photosphere, The Sun, edited by G. P. Kuiper, University of Chicago Press, Chicago, 88-177, 1953.
- Radio Corporation of America, RCA Photosensitive Devices and Cathode Ray Tubes, Radio Corporation of America, Harrison, New Jersey, 1-31, 1958.
- Rougier, G., Photoelectric Color Index of the Moon, Ann. Obs. Strasbourg, 3, 257-260, 1937.
- Stebbins, J., and G. E. Kron, The Stellar Magnitude and Color Index of the Sun, Astrophys. J., 126, 266-28-, 1957.
- Walsh, J. W. T., Photometry, Constable and Company Ltd., London, Appendix IV, 1953.
- Willey, R. L., and H. A. Pohn, Detailed Photoelectric Photometry of the Moon, in preparation, 1964.
- Willey, R. L., and B. C. Murray, Ten Micron Stellar Photometry - First Results and Future Prospects, Colloque International d'Astrophysique tenu a l'Universite de Liege, Tome IX, 460-468, 1964.

TABLE I

Julian Day	Longitude Sub- Mariner Point (°)	Latitude Sub- Mariner Point (°)	Earth's Phase-Angle (°)	Range 10 <sup>4</sup> Km	T(°F)	Ft-Candles at 1 A. U.
2437937+						
0.111	2	-1.9	45.2	860	91.5	1.50 × 10 <sup>-6</sup>
0.113	359	-1.9	45.1	861	91.5	1.57
0.127	354	-1.9	45.0	862	91.5	1.65
0.179	339	-1.9	45.0	863	91.5	1.73
0.218	334	-1.9	44.9	864	91.5	1.84
0.288	306	-1.9	44.8	866	91.5	1.96
0.371	284	-1.9	44.7	867	91.5	1.85
0.427	254	-1.9	44.7	868	91.5	1.75
0.517	216	-1.9	44.6	869	91.5	1.68
0.592	189	-1.9	44.6	871	91.5	1.76
0.644	171	-1.9	44.5	872	91.5	1.88
0.811	111	-1.9	44.3	875	91.5	2.09
1.034	30	-1.9	44.0	880	91.7	2.03
1.246	312	-1.9	43.8	883	91.8	2.14
1.370	268	-1.9	43.7	889	91.9	2.08
1.468	264	-1.9	43.5	892	91.9	1.98
1.640	50	-1.9	43.2	899	92.0	2.23
2.049	22	-1.9	42.9	906	91.7	2.03
2.085	10	-1.9	42.8	908	91.3	2.15
2.267	304	-1.9	42.6	912	91.0	2.27
2.427	247	-1.9	42.4	916	90.7	2.18
2.481	227	-1.9	42.3	917	90.3	2.04
2.543	204	-1.9	42.2	919	90.0	2.17
2.558	199	-1.9	42.1	920	90.0	2.27
2.571	194	-1.9	42.1	920	90.5	2.18
2.755	128	-1.9	42.0	925	91.0	2.32
3.199	327	-1.9	41.5	937	91.5	2.30
3.503	217	-1.9	41.1	944	92.0	2.45
3.586	187	-1.9	41.0	946	92.0	2.35
3.740	132	-1.9	40.8	950	92.0	2.49
3.908	71	-1.9	40.6	955	92.0	2.40
4.200	326	-1.9	40.3	962	92.0	2.54
4.435	241	-1.9	40.0	967	92.0	2.46
4.556	197	-1.9	39.8	971	92.0	2.34
4.736	132	-1.9	39.7	976	92.0	2.62
4.820	102	-1.9	39.5	978	92.0	2.51
4.913	68	-1.9	39.4	981	91.7	2.38
5.038	23	-1.9	39.2	984	91.3	2.52
5.205	323	-1.9	39.1	988	91.0	2.65
5.385	258	-1.9	38.9	993	90.7	2.55
5.704	142	-1.9	38.5	1002	90.3	2.44
6.062	13	-1.9	38.1	1010	90.0	2.61
6.126	351	-1.9	37.9	1013	90.0	2.48
6.143	344	-1.9	37.9	1013	89.8	2.63
6.161	338	-1.9	37.9	1014	89.6	2.48
6.268	293	-1.9	37.8	1017	89.4	2.64
6.435	233	-1.9	37.6	1020	89.2	2.49
6.600	179	-1.9	37.4	1024	89.0	2.35
6.737	129	-1.9	37.3	1027	88.7	2.51
6.833	94	-1.9	37.1	1031	88.3	2.37

(2)

7.176	330	-1.9	36.7	1041	88.0	2.56
7.500	213	-1.9	36.3	1049	87.7	2.43
7.708	139	-1.9	36.1	1055	87.5	2.35
7.965	48	-1.9	35.7	1061	87.3	2.48
8.213	316	-1.9	35.4	1069	87.0	2.66
8.408	246	-1.9	35.3	1073	86.7	2.52
8.479	220	-1.9	35.1	1075	86.3	2.41
8.602	175	-1.9	35.0	1078	86.0	2.31
8.876	76	-1.9	34.6	1086	86.3	2.46
9.194	321	-1.9	34.3	1095	86.7	2.63
9.362	260	-1.9	34.1	1099	87.0	2.53
9.455	227	-1.9	34.0	1101	87.3	2.44
9.559	189	-1.9	33.9	1104	87.7	2.34
9.686	144	-1.9	33.7	1108	88.0	2.49
9.885	71	-1.9	33.3	1115	87.9	2.64
10.100	354	-1.9	33.1	1119	87.8	2.77
10.166	330	-1.9	33.0	1121	87.7	2.96
10.220	310	-1.9	32.9	1122	87.6	2.79
10.304	280	-1.9	32.8	1124	87.4	2.68
10.362	260	-1.9	32.7	1126	87.3	2.55
10.538	196	-1.9	32.6	1133	87.2	2.46
10.788	106	-1.9	32.3	1138	87.0	2.60
10.949	47	-1.9	32.1	1142	87.0	2.74
11.174	326	-1.9	31.8	1150	87.0	2.90
11.279	288	-1.9	31.7	1152	87.0	2.79
11.293	284	-1.9	31.7	1153	87.0	2.68
11.592	175	-1.9	31.3	1162	87.0	2.59
11.866	75	-1.9	31.0	1170	87.0	2.62
11.907	61	-1.9	30.9	1171	87.0	2.88
11.988	32	-1.9	30.8	1173	87.0	2.77
12.126	342	-1.9	30.7	1177	87.0	2.91
12.708	132	-1.9	30.0	1195	87.0	2.74
13.130	339	-1.9	29.4	1205	87.0	2.88
13.358	257	-1.9	29.1	1213	86.7	2.81
13.971	35	-1.9	28.3	1231	87.5	2.90
14.407	238	-1.9	27.9	1243	86.3	2.79
14.465	217	-1.9	27.8	1246	85.8	2.69
14.538	190	-1.9	27.7	1248	85.5	2.79
14.956	39	-1.95	27.1	1261	85.4	2.92
15.347	259	-1.96	26.7	1272	85.3	2.90
15.443	224	-1.96	26.6	1274	85.2	2.79
15.541	187	-1.97	26.4	1279	85.0	2.91
15.871	68	-1.98	26.0	1288	85.0	3.12
16.230	298	-1.99	25.6	1300	85.0	3.03
16.431	226	-1.99	25.4	1305	85.0	2.92
16.604	164	-2.00	25.2	1311	85.0	3.07
16.678	137	-2.00	25.1	1314	85.0	3.25
16.767	105	-2.00	25.0	1316	85.0	3.08
16.824	85	-2.00	24.9	1318	85.0	2.94
16.973	30	-2.01	24.8	1323	85.0	3.13
17.137	331	-2.02	24.6	1328	85.0	3.15
17.184	314	-2.03	24.5	1330	85.0	3.32
17.211	304	-2.04	24.4	1331	85.0	3.16
17.783	99	-2.05	23.8	1348	85.0	3.10
18.356	251	-2.05	23.1	1368	85.0	3.07

(3)

18.428	225	-2.06	23.0	1371	85.0	2.93
18.505	196	-2.07	22.9	1373	85.0	3.09
18.881	61	-2.08	22.5	1386	85.0	3.30
19.263	282	-2.11	22.0	1398	85.0	3.17
19.395	220	-2.11	21.8	1402	85.0	3.16
20.132	329	-2.11	21.0	1427	84.9	3.17
20.444	216	-2.1	20.7	1437	84.7	3.20
20.673	132	-2.2	20.4	1446	84.4	3.39
21.090	343	-2.2	20.0	1461	84.0	3.32
21.458	210	-2.2	19.6	1473	84.0	3.26
21.833	74	-2.2	19.1	1487	84.0	3.41
26.301	261	-2.50	15.5	1616	83.0	3.52
26.493	192	-2.52	15.4	1625	82.5	3.30
26.697	118	-2.53	15.2	1632	82.0	3.34
26.966	20	-2.56	15.0	1636	82.0	3.34
27.068	284	-2.59	14.8	1654	82.0	3.67
27.399	224	-2.62	14.7	1660	82.0	3.44
27.823	71	-2.66	14.3	1677	82.0	3.38
28.073	341	-2.67	14.1	1686	82.0	3.55
28.198	295	-2.68	14.0	1693	82.0	3.82
28.241	279	-2.68	13.9	1698	82.0	3.60
28.467	199	-2.71	13.8	1704	82.0	3.51
28.698	116	-2.72	13.6	1714	82.0	3.41
28.948	24	-2.75	13.4	1724	82.0	3.60
29.097	302	-2.78	13.3	1734	82.0	3.73
29.333	245	-2.79	13.2	1741	82.0	3.64
29.435	209	-2.80	13.1	1744	82.0	3.53
29.687	117	-2.83	12.9	1756	82.0	3.43
29.908	22	-2.85	12.7	1767	82.0	3.62
30.132	317	-2.80	12.6	1775	82.0	3.80
30.305	253	-2.89	12.5	1783	82.0	3.68
30.694	113	-2.94	12.4	1800	82.0	3.61
31.111	321	-2.97	12.2	1818	82.0	3.83
31.257	269	-2.98	12.1	1826	82.2	3.70
31.406	216	-2.99	12.1	1830	82.5	3.63
31.492	186	-3.01	12.0	1835	82.8	3.51
31.543	171	-3.03	11.9	1838	83.0	3.64
31.630	136	-3.05	11.9	1881	82.8	3.75
31.811	71	-3.07	11.8	1850	82.5	3.72
32.032	350	-3.09	11.8	1860	82.3	3.83
32.201	288	-3.23	11.4	1915	82.0	3.85
32.281	259	-3.24	11.4	1918	82.7	3.63
32.785	77	-3.32	11.4	1942	83.3	3.49
33.295	252	-3.38	11.4	1966	84.0	3.41
33.471	189	-3.41	11.3	1977	84.0	3.25
33.641	127	-3.5	11.3	1986	84.0	3.49
33.883	39	-3.5	11.3	1997	84.1	3.35
34.214	280	-3.5	11.3	2014	84.2	3.49
34.333	238	-3.5	11.3	2020	84.3	3.34
34.431	203	-3.5	11.3	2024	84.4	3.17
34.525	167	-3.5	11.3	2029	84.5	3.37
34.636	127	-3.5	11.3	2034	84.6	3.49
34.753	86	-3.5	11.4	2040	84.6	3.42
34.818	64	-3.5	11.4	2044	84.7	3.24
34.894	34	-3.5	11.4	2048	84.7	3.45
35.031	345	-3.5	11.4	2055	84.8	3.57

(4)

35.169	296	-3.6	11.4	2063	84.8	3.50
35.239	270	-3.7	11.4	2066	85.0	3.32
35.314	243	-3.7	11.4	2070	85.0	3.23
35.434	201	-3.8	11.4	2076	85.2	3.05
35.533	164	-3.8	11.5	2082	85.4	3.28
35.639	125	-3.8	11.5	2089	85.5	3.39
35.730	92	-3.8	11.5	2093	85.6	3.32
35.815	62	-3.8	11.6	2097	85.6	3.14
35.909	28	-3.8	11.6	2100	85.7	3.36
36.028	345	-3.8	11.6	2107	85.7	3.44
36.192	285	-3.8	11.7	2117	85.8	3.52
36.265	259	-3.8	11.7	2120	85.9	3.41
36.385	216	-3.9	11.7	2126	86.0	3.25
36.739	88	-3.9	11.9	2140	86.0	3.29
37.042	339	-3.9	12.0	2160	86.5	3.58
38.107	314	-4.0	12.5	2220	87.0	3.34
38.410	206	-4.1	12.6	2230	88.0	3.30
38.773	76	-4.2	12.8	2250	89.0	3.15
38.850	45	-4.2	12.9	2260	89.5	3.31
39.044	336	-4.2	13.0	2270	90.0	3.33
39.244	263	-4.2	13.1	2280	90.0	3.39
39.398	244	-4.2	13.2	2290	90.5	3.32
39.352	225	-4.2	13.2	2290	91.0	3.22
39.447	191	-4.2	13.3	2300	91.5	3.14
39.556	149	-4.3	13.4	2300	92.0	3.25
39.627	125	-4.3	13.4	2310	92.2	3.44
39.684	105	-4.3	13.4	2310	92.4	3.32
39.750	81	-4.4	13.4	2320	92.6	3.24
39.848	45	-4.4	13.5	2320	92.8	3.35
39.979	358	-4.4	13.6	2330	93.0	3.53
41.153	294	-4.5	14.4	2400	93.0	3.17
41.185	281	-4.6	14.4	2400	93.5	3.07
41.441	190	-4.6	14.5	2410	94.0	2.95
41.760	74	-4.7	14.8	2440	95.0	2.88
41.845	43	-4.7	14.9	2450	95.3	2.94
41.935	11	-4.7	14.9	2450	95.7	3.11
42.031	342	-4.8	15.0	2460	96.0	3.05
42.310	236	-4.8	15.2	2470	96.5	3.02
42.579	138	-4.8	15.4	2490	97.0	2.83
42.644	115	-4.8	15.5	2500	97.3	2.86
42.715	90	-4.9	15.5	2500	97.5	2.78
42.752	76	-4.9	15.6	2510	97.8	2.70
42.799	60	-4.9	15.6	2510	98.0	2.79
42.989	350	-4.9	15.8	2520	98.2	2.89
43.192	276	-5.0	15.9	2530	98.4	2.87
43.382	208	-5.0	16.0	2540	98.6	2.78
43.553	146	-5.0	16.2	2550	98.8	2.70
43.763	70	-5.1	16.3	2570	99.0	2.69
44.007	345	-5.1	16.5	2590	99.5	2.83
44.075	318	-5.1	16.5	2590	100.0	2.76
44.229	262	-5.2	16.6	2600	100.5	2.80
44.371	211	-5.2	16.8	2610	101.0	2.69
44.506	162	-5.2	16.9	2620	101.5	2.63
44.647	112	-5.2	17.0	2630	102.0	2.58

(5)

44.726	83	-5.3	17.1	2630	102.1	2.37
44.807	54	-5.3	17.2	2640	102.2	2.60
45.011	341	-5.3	17.3	2650	102.4	2.76
45.218	264	-5.4	17.4	2670	102.5	2.69
45.328	225	-5.4	17.6	2680	102.7	2.51
45.845	39	-5.5	18.0	2710	102.8	2.37
46.277	238	-5.6	18.3	2750	103.0	2.34
46.496	160	-5.6	18.5	2760	104.5	2.36
46.730	80	-5.7	18.6	2770	106.0	2.34
47.032	330	-5.7	19.0	2800	106.3	2.51
47.326	225	-5.7	19.1	2820	106.7	2.44
47.399	198	-5.8	19.2	2820	107.0	2.36
47.465	174	-5.8	19.3	2830	107.3	2.31
47.569	136	-5.9	19.3	2830	107.7	2.27
47.715	84	-5.9	19.5	2840	108.0	2.23
47.780	61	-6.0	19.5	2850	108.3	2.22
48.081	312	-6.0	19.8	2870	108.6	2.41
48.459	174	-6.0	20.1	2910	108.8	2.27
48.518	153	-6.1	20.1	2910	109.0	2.18
48.666	100	-6.2	20.3	2920	109.3	2.30
48.986	345	-6.2	20.6	2940	109.7	2.38
49.197	268	-6.2	20.7	2960	110.0	2.61
49.232	256	-6.2	20.8	2960	110.5	2.59
49.309	228	-6.2	20.8	2970	111.0	2.56
49.458	174	-6.3	20.9	2980	111.5	2.31
49.527	149	-6.3	21.0	2980	111.5	2.32
49.572	133	-6.3	21.0	2980	111.7	2.26
49.638	109	-6.3	21.1	2990	111.8	2.23
49.708	94	-6.3	21.1	3000	111.9	2.32
49.878	23	-6.4	21.2	3010	112.0	2.42
50.086	309	-6.4	21.3	3020	112.2	2.54
50.159	282	-6.4	21.4	3030	112.3	2.57
50.187	271	-6.5	21.5	3030	112.4	2.69
50.275	239	-6.5	21.6	3030	112.6	2.49
50.397	196	-6.5	21.7	3040	112.7	2.39
50.461	172	-6.5	21.8	3060	112.8	2.32
50.534	146	-6.5	21.8	3060	112.9	2.22
50.635	111	-6.6	21.9	3070	113.0	2.36
50.739	72	-6.6	21.9	3080	113.5	2.49
51.032	328	-6.7	22.1	3100	114.0	2.71
51.288	235	-6.7	22.4	3120	114.5	2.64
51.318	224	-6.7	22.4	3130	115.0	2.56
51.600	121	-6.7	22.7	3140	115.2	2.54
52.052	319	-6.8	22.9	3180	115.5	2.80
52.281	239	-6.9	23.0	3210	115.7	2.63
52.340	213	-6.9	23.1	3210	116.0	2.53
52.399	192	-7.0	23.2	3210	116.3	2.51
52.458	171	-7.0	23.4	3220	116.5	2.53
52.618	113	-7.0	23.5	3230	116.7	2.60
53.000	336	-7.1	23.7	3270	117.0	2.83
53.254	245	-7.2	23.9	3290	117.5	2.73
53.288	233	-7.2	24.0	3290	118.0	2.71
53.538	142	-7.2	24.1	3310	118.5	2.74
53.817	26	-7.3	24.4	3340	119.0	2.93